

Hydrochemical characterization of groundwater in the Continental Terminal aquifer of Moundou and its surroundings (southwestern Chad).

Abstract

The aim of our study is to characterize the physicochemical and bacteriological parameters of groundwater in and around the town of Moundou. The water in this locality is contained in continental-terminal formations and consists exclusively of sand and sandstone. Two campaigns carried out in December 2023 and March 2024 collected sixty (60) samples. Forty (40) samples were used for physicochemical analyses (iron, zinc) and twenty (20) for bacteriological analyses (faecal and total coliforms, total aerobic mesophilic flora, *Escherichia coli* and total germs). Results for physico-chemical parameters indicate that these waters are acidic (pH between 6.3-6.94), and that their mineralization is due to both natural and anthropogenic factors. Groundwater in the study area is dominated by calcium-magnesium bicarbonate facies, followed by calcium-magnesium chloride-sulfate facies. GWQI values range from 19.37 to 78.48, indicating that these waters are excellent and of good physico-chemical quality for human consumption, although the mineralization is the result of anthropogenic action. However, the bacteriological study shows that surface and deep groundwater are of poor quality and require filtration and disinfection before consumption.

Key words: Moundou, groundwater, characterization, Continental Terminal, Hydrochemistry.

Introduction

Essential for life and health (Niambele *et al.*, 2020; WHO, 2011; Adetunde *et al.*, 2011, WHO and UNICEF, 2018; Diallo, 2017), water plays an active role in agricultural and industrial development and energy production. The body of an adult human being, being 60% water, requires a minimum consumption of 1.5 liters of water per day (DIOP, 2006). However, one of the causes of various human pathologies results from the consumption of polluted and/or contaminated water (Haslay and Leclerc, 1993; Adetunde *et al.*, 2011; Dovonou *et al.*, 2011; Adesakin *et al.*, 2020; WHO & UNICEF, 2018; Ounokis and Achour, 2014). Estimated at 15.9 million km³ (Ferguson *et al.*, 2021), the world's water reserves are heavily exploited, with groundwater reserves estimated to account for around 40% of the total volume (Van der Gun, 2022), making them the most heavily exploited (Margat, 2019). Thus, it is clear that the quality of drinking water depends on its physico-chemical and bacteriological characteristics (Adesakin *et al.*, 2020; Sila, 2019; Esharegoma *et al.*, 2018; Bello *et al.*, 2013; Okoli, 2012).

In Chad, groundwater is the most consumed at 65% (INSEED, 2015). According to UNICEF (2019), 22% of children under 5 suffer from diarrheal diseases caused by contaminated water. Chad's Ministry of Water supports this assertion, concluding that waterborne diseases represent the second leading cause of child mortality and morbidity after malaria (MEEP, 2019).

The health issue linked to the consumption of poor quality water remains a concern in Moundou and the surrounding area. According to the African Development Bank (2015), only 36.5% of local residents have access to drinking water, compared with 53% nationally, while the components national and study area sanitation each cover 16% (PAEPA 2015). This is why it is important to be able to characterize the physico-chemical parameters of water from wells and boreholes, as well as from conveyance systems, in order to gain a better understanding of

contamination mechanisms and develop protection strategies in line with the recommendations of previous studies (Fehdi *et al.*, 2009 ; Bouchemal *et al.* 2015 ; Gnazou, 2015).

I.1 Introduction to the study area

I.1.1 Geographical, climatic and economic context of the study area

Belonging to the Western Logone Province, the study area is located in south-western Chad, some 480 km from the capital N'Djaména, between 8°28'27.40"-8°41'51.59" north latitude and 15°55'19.34"-16°10'6.85" east longitude (Fig.1). The area covers 230 km² with an estimated 2020 population of 347,058 (INSEED, 2020). The altitude of the study area ranges from 377 to 498 m. The soudanian climate of the study area is punctuated by the Front Inter Tropical (BRGM, 1992 ; Djoret, 2000). This results from the clash between the Harmatan, hot, dry air from the Saharan high-pressure zone to the north, and the monsoon, humid air from the Atlantic. Climatic data for Moundou and the surrounding area (rainfall and temperatures) combined for the period 1980 to 2019 (ANAM, 2019), are characteristic of the two seasons usually highlighted in this type of climate : a dry period extending from November to April and a wet period extending from May to October, with a concentration of rainfall in July and August (Fig.1).

The income of the majority of the population comes, on the one hand, from the exploitation of the land through the cultivation of cash crops such as food crops and market gardening, and on the other hand, from the products of poultry and small livestock farming. Fishing and hunting are of great social and economic importance, also as a source of subsistence and income. The industrial sector is represented by Société Cottonnière du Tchad for cotton ginning, Brasseries du Tchad (BDT) for beverage production and marketing, and Complexe Industriel des Abattoirs du Logone (CIAL) for meat exports to neighboring countries, the usine de l'huilerie-savonnerie for vegetable oil production, the Sociétés Tchadienne d'Eau (STE) and Nationale d'Electricité (SNE) responsible for the production, transport and distribution of drinking water and electricity, not forgetting bakeries.

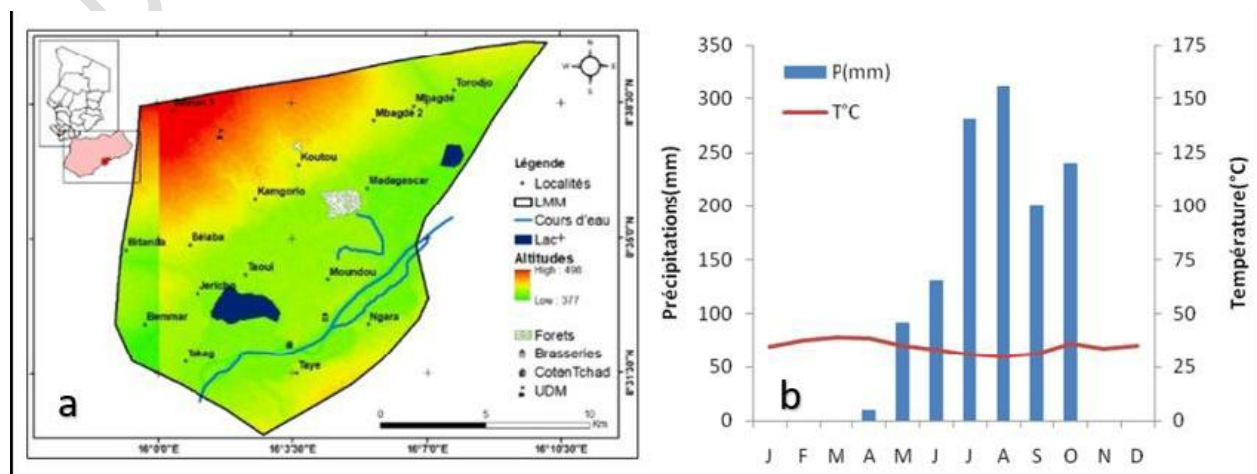


Figure0 : Location of the study area in Chad (a) and umbrothermal diagram (b) of the study area.

Belonging to the Doba-Salamat basin, the formations in the study area date from the continental terminal and are made up of sand and sandstone with criss-cross stratification, versicolored clays, kaolin lenses and concretionary or pisolithic ferruginous levels (BRGM, 1992 ; SDEA, 2003). In terms of hydrogeology, authors (Garin, 1979 ; Wolf, 1992) have shown that the aquifer in the study area is made up of fine and coarse sand. This is confirmed by recent drilling work carried out by the Ministry of Water and Sanitation, showing an area made up of sedimentary formations (sands, clayey sandstones, sandy clays and argillites) and residual formations (lateritic cuirasses). (Fig.3). The aquifer is mainly recharged by rainwater (BRGM, 1987). The piezometric surface of the aquifer is shallow (what?? you have to specify shallow??), less than 10 m above ground level in the valleys (BRGM,1987, SDEA,2003). However, it can exceed 80 m in the plateau sector, particularly in the Koros region (Fig.2).

Figure 2: Lithological cross-section of boreholes (source, MAE,2013)

I.2.1 Field work

It took place at the Logone Occidentale health delegation, and involved oral questions followed by notes. The oral interview with the head of health statistics enabled us to gather information on water-borne diseases frequently diagnosed and treated in health centers and hospitals in and around Moundou.

- Piezometric and hydrochemical monitoring

- Piezometric monitoring

Piezometric monitoring is carried out during two campaigns : IL a firstcampagne s'est déroulées in December 2023 andla seconde in March 2024. Static levels will be measured using a dual-signal (sound and light) 150-meter piezometer. To measure piezometric levels, place the probe on the well's curbstone andla unroll the tape. When the lower end of the electrode touches the water surface, the luminous and audible indicators are activated, On thus enablingread lit done to directly the distance Z_p , which corresponds to the distance between the water surface in the well and the upper level of the coping in metres. Then, using the same piezometer probe tape, we measure the height of the coping (H_m). Then, using a *Garmin* GPS (Global Positioning System) receiver, the geographical coordinates of the various structures concerned are recorded by placing it on the upper edge of the coping. All these data are carefullysaignement marked on a(Tab.1) data collection sheet (Tab.1).

Table 1: Example of a piezometric monitoring sheet

Type of structure	Coordonnée géographiques			Z_p	H_m	quartier
	X	Y	Z			
Well	16,4	8,51	411	13,8	1,3	Doumber 3
drilling	16,01	8,52	421	38	2	Doumber 1

- Hydrochemical monitoring of water points

Hydrochemical monitoring is carried out in two campaigns, one during high-water periods (December 2022) and the other during low-water periods (March 2024). For each campaign, we collected thirty (30) water samples, including twenty (20) for physico-chemical analysis and ten (10) for bacteriological analysis (Fig.3). Water samples were taken from selected structures only, using 1.5-liter PVC bottles previously cleaned and washed with distilled water. A total of sixty water samples were collected pour les deux campagnes (during periods low and high water). All samples were analyzed at the Brasseries de Moundou hydrochemical laboratory. Temperature ($^{\circ}\text{C}$), Hydrogen Potential (pH), Conductivity ($\mu\text{S}/\text{cm}$), Total Dissolved Solid (mg/l) were measured *in situ* using a Hanna *HI 9813-5* multi-parameter water tester, previously cleaned and calibrated in the laboratory.

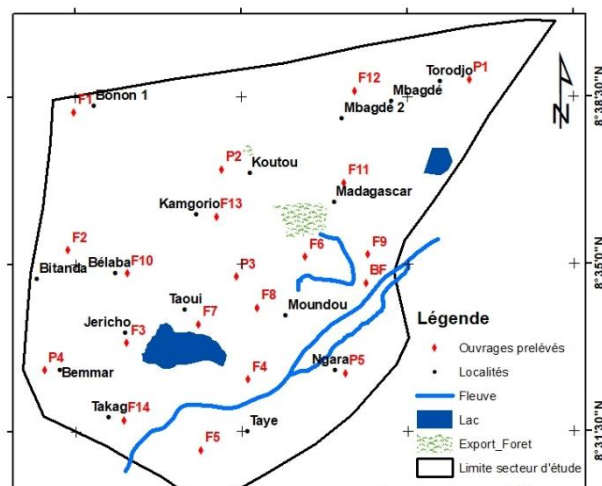


Figure 3: Map of water sampling points

I.2.2 Laboratory work

- **Physico-chemical and bacteriological water analysis**

- ☐ **Physico-chemical analysis**

- Turbidity assessment

It was evaluated using a *Haffmans VOS ROTA 90* turbidimeter. The operation is performed as follows:

- rinsing the glass with the water to be tested
- pour the water into the glass and place in the *Haffmans VOS ROTA 90* ;
- press the Start button ;
- playback.

- ☐ Concentrations of magnesium (Mg^{2+}), sodium (Na^{+}) and potassium (K^{+}), calcium(Ca^{2+}) , sulfate(SO_4^{2-}) , nitrate(NO_3^{-}) , nitrite (NO_2^{-}) , phosphate (PO_4^{3-}) were determined using a *LANGE DR6000* Photometer. Iron (Fe), lead (Pb^{2+}), zinc (Zn^{2+}) , chloride (Cl^{-}) were measured using a *NOVA 60* spectroquant. Bicarbonate (HCO_3^{-}), and silica were determined by titration.

- ☐ Calculate GWQI (Ground Water Quality Index)

GWQI was calculated as follows:

- ☐ Assigning a weight to each parameter according to its importance on water quality and its effect on health (Elkhalki *et al.*,2023) on a scale of 1 to 5 (Tab.3);

- ☐ Calculation of the relative weight (W_i) à partir de according to the following equation from the data $\frac{w_i}{\sum_{i=1}^n w_i}$, $W_i = \frac{w_i}{\sum_{i=1}^n w_i}$ with W_i = relative weight and w_i = weight of each parameter; n = number of parameters.

- ☐ calculation of q_i for each parameter by dividing its concentration for each sample by its limit value (standard) set by the WHO (2017) multiplied by 100 as indicated by the equation : $q_i = \frac{C_i}{S_i} * 100$

C_i = concentration of each chemical parameter in each water sample in mg/l ;

S_i = the sum of the weights assigned to the parameters according to the WHO standard (2017).

- ☐ Bacteriological analysis

The bacteriological analysis was carried out in four phases :

i) preparation of culture media - *ii)* inoculation - *iii)* incubation - *iv)* colony counting.

- ☐ Preparation of culture media

Three culture media (chromocult, Stlanetz and Barthey) were prepared in the host :

- Chromocult medium: 3.37 g of chromocult (C) dissolved in 125 ml of distilled water was heated in a boiling flask with regular stirring until the chromocult was completely dissolved forpendant 24 to 48h at a temperature of 37°C. En suite After cooling, the solution was poured into a sterile petri dish (10-15ml). This medium is used to determine bacteria such as total Coliforms, *Escherichia coli* and thermo-tolerants.

- Slanetz and Barthey medium: 5.25g of Slanetz dissolved in 125ml of distilled water was heated in a boiling flask over a fire, stirring until the medium was completely dissolved. The resulting solution was then cooled and 2.5ml of TTC added before transferring to the petri dish. The culture lasts 48 hours at a temperature of 37°C, and enables fecal enterococci to be determined.

- Plate Count Agar (PCA) medium: 2.18g PCA dissolved in 125ml distilled water and heated in an autoclave at 121°C. The resulting solution was cooled and then poured into the petri dish. The bacteria sought in these media are total aerobic flora. Bacteria are counted ats after 48 hours incubation at 37°C.

□ Filtration plating: this stage of bacterial determination was carried out under aseptic conditions in the host, to avoid any kind of contamination that might influence the results. Thus 100 ml of sample water was filtered with a vacuum pump through a 0.4µm membrane which is placed on a filter paddle. After filtration, the membrane was placed on a petri dish containing nutrients for bacterial germs.

□ **Counting bacteria** : Colony counting on selective media is carried out using a colony counter. Each colony is marked with an indelible marker on the reverse side of the petri dish. Typical *Escherichia coli* colonies are dark blue to violet, total coliforms are brown on medium C (Chromocult), fecal enterococci are brown on medium S (Slanetz) and aerobic flora are brown on medium PCA.

III.3.2.2. Drawing diagrams

Diagrams such as Piper's, Stiff's and Korjinski's were produced using the Hydrochimique d'Avignon 5.3 software, based on physico-chemical data. These data were first entered into a Microsoft Excel spreadsheet and then exported to the hydrochemical software. On the other hand, the Gibbs diagram, umbrothermal diagram and histograms were produced in Microsoft Excel.

III.3.3. Processing of hydrochemical data

The results of the physico-chemical analyses were processed using the multivariate statistical analysis method and the hydrochemical method. The hydrochemical method consisted in using the Piper diagram, the Korjinski diagram, under the Hydrochimique d'Avignon 5.3 software, as well as the Gibbs diagram under Excel. The piper diagram is used to determine the chemical facies of the water, while the Korjinski diagram is used to determine the existence of any silicate alteration. The Gibbs diagram can be used to determine the origins of water mineralization. The multivariate statistical analysis method is based on the use of Principal Component Analysis (PCA) under R studio software. PCA is used to understand the phenomena behind the mineralization of groundwater ions

III.3.4. Results and interpretation

The results of physico-chemical and bacteriological analyses were discussed by comparison with WHO (2017) standard values for water intended for human consumption.

RESULTS

□ Inventory of water production facilities

Findings in the field showed that the most commonly used groundwater exploitation structures in the study area are boreholes fitted with human-powered or submerged apples, and roughly landscaped wells. The vast majority of these structures have a dirty environment (presence of stagnant water containing debris of all kinds).

□ Health survey

Surveys carried out in the Logone Occidental health delegation, ont ont recueillies sur reveal three (03) main water-borne diseases in the study area: diarrhoea, typhoid fever and cholera. Only the first two (02) are frequently encountered in the locality (Tab.2). The data in this table show that over the last ten years no cases of cholera have been recorded, whereas typhoid fever and diarrhoea peaked in 2018 and 2021 respectively

Period	Typhoid fever	Diarrheal diseases	Cholera	Period	Typhoid fever	Diarrheal diseases	Cholera
2015	450	300	0	2020	564	7201	0
2016	259	379	0	2021	749	8484	0
2017	214	3658	0	2022	597	3089	0
2018	467	17448	0	2023	334	2802	0
2019	349	16211	0	2024	445	2226	0
2020	564	7201	0	2020	564	7201	0
2021	749	8484	0	2021	749	8484	0
2022	597	3089	0	2022	597	3089	0
2023	334	2802	0	2023	334	2802	0
2024	445	2226	0	2024	445	2226	0

Source : Délégation Sanitaire du Logone Occidental (2024).

■ Piezometry of the city of Moundou and its surroundings

The piezometric maps drawn up from data collected during low and high-water periods highlight two piezometric domes. The 1st dome is located to the west and the second to the north of the study area. From the 1st, groundwater flows from the central west towards the north, east and south, while from the 2(nd), groundwater flowsnt towards the north and east, accumulating in piezometric depressions located to the south and east beneath the Logone River (Fig.4).

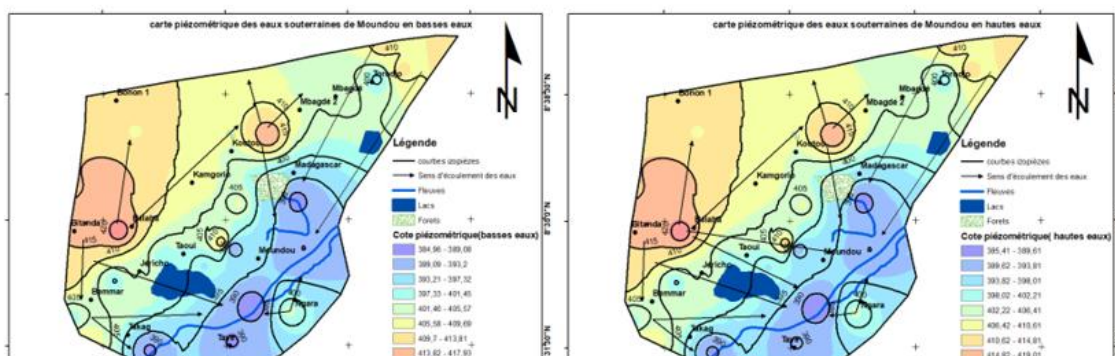


Figure 4: Piezometric map of Moundou and surrounding area at low(a) and high(b) water levels.

IV.4. Physico-chemical parameters measured in situ

IV.4.1. pH of water during low and high water periods

In the low-water period, well water pH values range from 5.78 (P2) to 6.46 (P1), with a mean of 6.16 and a standard deviation of 0.2. In the high-water period, pH values range from 5.98 (P2) to 6.79 (P4), with a mean of 6.44 and a standard deviation of 0.34 (Tab.3). Well water is acidic and does not comply with the WHO standard (2017). During low-water periods, well water pH values range from 5.09 (F5) to 6.91 (F12), with a mean of 6.06 and a standard deviation of 0.58, whereas during high-water periods, they range from 5.19 (F5) to 6.98 (F10), with a mean of 6.32 and a standard deviation of 0.59 (Tab.3).

Table 3: Variations in groundwater conductivity

water points		well		Drilling		Fountain terminals	
Parameter		pH					
Sampling period		Low	High	Low	High	Low	High
Statistical parameters	Mini.	5,78	5,98	5,09	5,19	1,88	0.9
	Max.	6,46	6,79	6,91	6,98	1,88	0.9
	Means.	6,16	6,44	6,06	6,32	1,88	0.9
	T. gap	0,25	0,34	0,58	0,59	0,00	0,00
WHO standard(2017)		6,5 -8,5					

IV.4.2. Water temperature

Well water temperatures range from 27.90°C (P3) to 29.5°C (P2), with an average of 28.66 and a standard deviation of 0.57, while at high water they oscillate between 27.80°C (P3) and 28.5°C (P2), with an average of 28.20 and a standard deviation of 0, (Tab.4). Borehole temperature values range from 26.9°C (F9) to 29.1°C (F11), with a mean of 28.06°C and a standard deviation of 0.64 in low water, and from 26.7°C (F10) to 28.5°C (F12), with a mean of 27.46 and a standard deviation of 0.56 in high water (Tab. 4). Values do not meet the WHO standard (2017). The temperature value is 29.3°C at low water and 28.2°C at high water for the hydrant water. These values exceed non conformes the standard recommended by the WHO (2017).

Table 4: Groundwater temperature variations

water points	well	Drilling	Fountain	water	well
--------------	------	----------	----------	-------	------

				terminals	points		
Parameter		Temperature					
Sampling period		Low	High	Low	High	Low	High
Statistical parameters	Mini.	27,90	27,80	26,90	26,70	29,3	28,2
	Max.	29,50	28,50	29,10	28,50	29,3	28,2
	Moy.	28,66	28,20	28,06	27,46	29,3	28,2
	Ecart T.	0,57	0,33	0,64	0,56	0,00	0,00
WHO standard(2017)	8-25						

IV.4.3. Groundwater conductivity

Electrical conductivity data (Tab.5) show low (21.5 $\mu\text{S}/\text{cm}$) and medium (309 $\mu\text{S}/\text{cm}$) values.

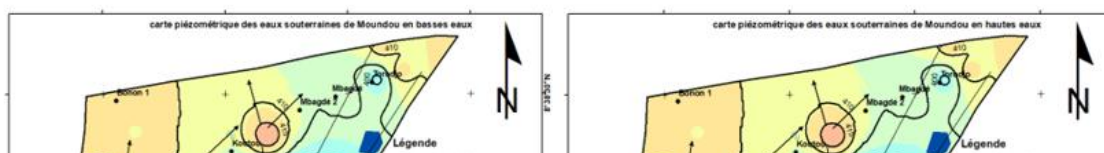
water points		well	Drilling	Fountain terminals	water points	well	
Parameter		Conductivity					
Sampling period		Low	High	Low	High	Low	High
Statistical parameters	Mini.	21,50	20,50	15,60	25,58	102	144,91
	Max.	309,00	409,00	302,00	309,00	102	144,91
	Moy.	121,02	144,42	88,54	112,61	102	144,91
	Ecart T.	113,85	156,87	71,13	83,71	0,00	0,00
WHO standard(2017)		2500					

IV.4.4. Groundwater turbidity at low and high water levels

Turbidity values (Tab.6) range from 0.09 (P4) and 44.10 (NTU) to 54.1 NTU, with well water being the most turbid.

Table 6: Variation in groundwater turbidity

water points		well	Drilling	Fountain terminals	water points	well	
Parameter		Turbidity					
Sampling period		Low	High	Low	High	Low	High
Statistical parameters	Mini.	0,09	1,60	0,38	1,51	1,88	0.9
	Max.	44,10	54,10	7,30	13,00	1,88	0.9
	Moy.	13,87	15,20	1,49	5,41	1,88	0.9
	Ecart T.	20,74	25,95	1,84	3,36	0,00	0,00
WHO	5 NTU						



standard(2017)	
----------------	--

IV.4.5. TDS of groundwater at low and high water levels

STD values range from 7.8 to 186 mg/l(Tab.7). These values are below the WHO standard (2017).

Table 7: Variation in groundwater STD.

water points	well		Drilling			Fountain terminals	
Parameter	TDS						
Sampling period		Low	High	Low	High	Low	High
Statistical parameters	Mini.	36,50	26,50	7,80	8,52	102,6	8,4
	Max.	153,00	179,00	168,00	185,00	102,6	8,4
	Moy.	75,54	79,70	53,89	64,69	102,6	8,4
	Ecart T.	45,89	59,25	45,95	50,98	0,00	0,00
WHO standard(2017)	500						

IV.5. Chemical parameters

Alkalis

Among the major cations, calcium is the dominant element, ensuite vient followed by sodium, then magnesium and finally potassium for boreholes. In wells, sodium predominates, ensuite followed by calcium, then potassium and finally magnesium. For alkalis, sodium is dominant in well and borehole water (in high water), then in hydrant water in high water, while potassium is dominant only in hydrant water and in borehole water in low water. All mean values for sodium and potassium in high-water hydrant water comply with the WHO (2017) pour les standard, i.e. water intended for human consumption.

Alkaline earths

The most abundant alkaline-earth element in groundwater in and around Moundou is calcium (Fig.5). Sodium is dominant in well and borehole water during both low- and high-water periods. In hydrant water, potassium dominates during low-water periods, while sodium predominates during high-water periods (Fig.5.a). Calcium is dominant in well and borehole water during both high and low water periods. In hydrant water, calcium dominates in both high and low water periods.

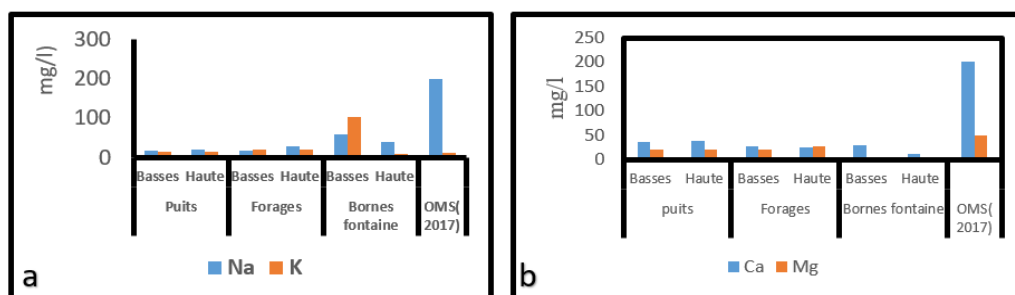


Figure 5. Alkali(a) and alkaline earth(b) content of groundwater

IV.5.6. Major anions

For major anions, bicarbonate (94.83 mg/l) predominates in all waters, followed by chloride in well water, while sulfate is second only to bicarbonate in borehole water (Fig.65). These average values are concordantes avec cellesde compliant with WHO (2017) guidelines for water intended for human consumption.

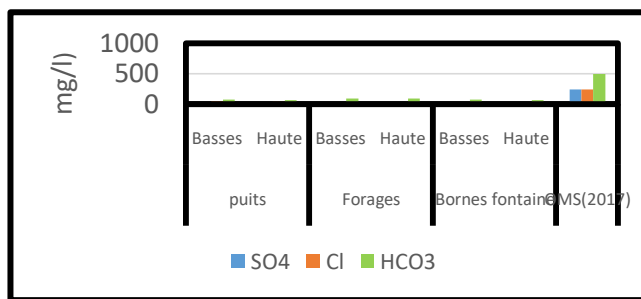


Figure 6: Major anion concentrations in groundwater

IV.5.7. Pollutants

Groundwater in the study area is dominated by nitrate compared with nitrite (Fig.76), followed by phosphate, but only the mean values for nitrite and phosphate are above the WHO standard value (2017).

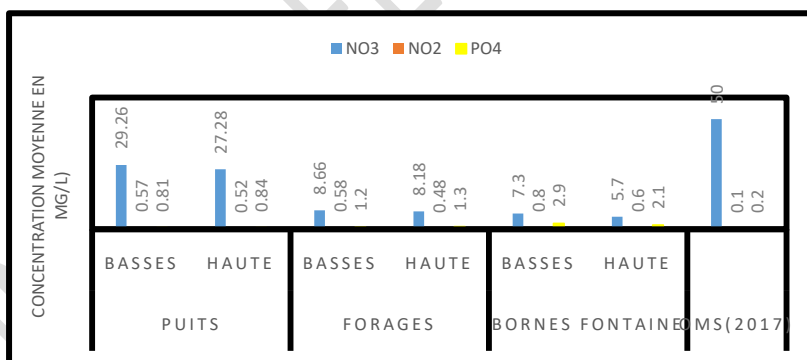
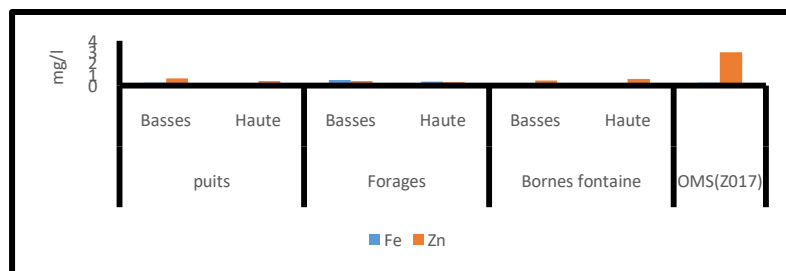


Figure 7: Pollutant levels in groundwater

IV.5.8. Trace metals

Concentrations of iron and zinc in groundwater in and around Moundou (Fig.7), with iron



predominating in borehole water at both high and low water levels, and zinc in well and standpipe water. Average iron values in borehole water are higher than the WHO guideline (2017) for water intended for human consumption.

Figure 7: Metal contents in groundwater

IV.5.9. Silica

The average silica value (Fig.8) decreases (38.8 to 113 mg/l) from well water through borehole water to standpipe water. These mean values are in their majority most cases higher than the WHO standard (2017), except for the hydrant water in low-water conditions.

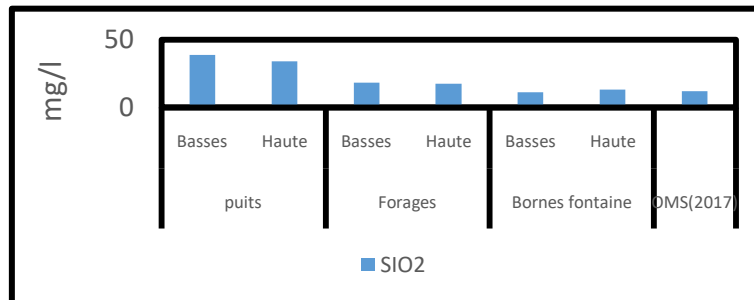


Figure 8: Silica levels in groundwater

IV.8. Hydrochemical facies of groundwater in and around Moundou

IV. 8.1. Water classification using the Piper diagram

The representation of chemical analysis results in the Piper diagram shows that groundwater in and around Moundou is dominated by the calcic carbonate facies (Fig.9). It can be seen that 35% of waters analyzed during low-water periods belong to the calcic-magnesium bicarbonate facies (F6, F12, F13, F8, P4, F14, F9), 25% to the calcic-magnesium chloride-sulfate facies (P1, P2, P5, F3, F5), 20% to sodium potassium bicarbonate facies (BF, F10, F11, F4), 15% to sodium potassium chloride or sodium sulfate facies (F7, F2, F1) and 5% to calcium bicarbonate facies (P3). In high water, 50% of the waters analyzed in low water periods belong to the calcic and magnesian bicarbonate facies (F6, F12, F13, F14, F4, F9, P3, F10, F8, P4), 25% to the calcic and magnesian chloride and sulfate facies (P2, F3, F1, P5, P1), 10% to the sodium and potassium carbonate facies (F11 and BF). 15% to the sodium potassium chloride or sodium sulfate facies (F5, F7, F2).

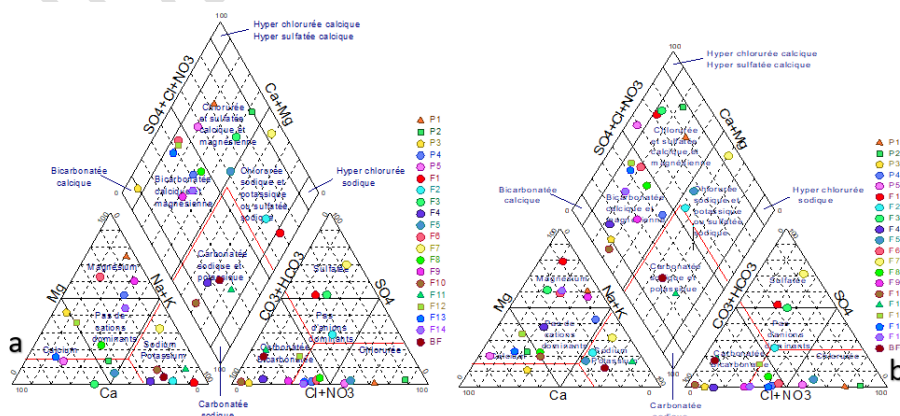


Figure 9: Hydrochemical facies of groundwater in low (a) and high (b) areas

IV.9. Principal component analysis (PCA)

PCA analysis of low-water data shows that factors 1 and 2 express 19.7% and 13.4% respectively, giving a total of 33.1% for both factors. In high water, the two factors account for 32.4% (16.7% for F1 and 15.7 for F2).

□ Low water (Fig.10.a)

The positive part of factor 1 is marked by parameters such as temperature, nitrate, chloride, conductivity, zinc, TDS and calcium. On the negative side, it is correlated with silica, turbidity, magnesium, pH and lead. Factor 2 is marked in its positive part by potassium, phosphate, sodium, bicarbonate, sulfate and nitrite; in its negative part, it is marked by iron only.

□ High water (Fig.10. b)

Factor 1 is marked by iron, TDS, Cl, conductivity, phosphate in its positive part and nitrate, silica, calcium, lead, temperature in its negative part.

Factor 2 is characterized in its positive part by magnesium, sodium, potassium and turbidity, while in its negative part it is marked by sulfate, bicarbonate, nitrite and zinc.

The correlation matrices highlight two types of correlation between the chemical

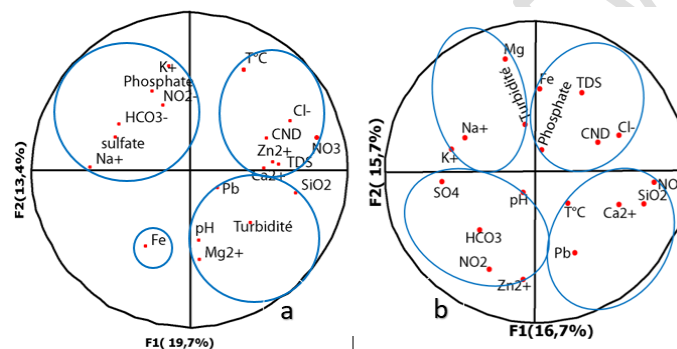


Figure 10 : Analysis of variables in the F1-F2 factorial plan in low water (a) and high water (b). elements. There is a significant correlation between some and a lesser one between others (Tab.8 and Tab.9).

In low water, conductivity correlates significantly with total dissolved solids (60%) and chloride (60%). Nitrate also correlates significantly with silica (55%) and chloride (57%). At high water levels, conductivity correlates significantly with TDS (60%) and chloride (58%).

An average correlation is observed between the chemical elements. These are STD and chloride (46%), temperature and potassium (42%), calcium and silica (44%) and sodium with sulfate and bicarbonate (45%) in low water. In high water (Tab 4.10), an average correlation is also observed. Temperature correlates on average with chloride and nitrate ($r=0.44$ and $r=0.47$ respectively). Turbidity is related to potassium and iron ($r=0.49$, $r=0.44$, respectively). An average correlation is observed between sodium and magnesium on the one hand, and sodium and potassium on the other (respectively $r=0.44$ and $r=0.42$). Potassium and bicarbonate (46%), silica with nitrate (47%) and lead(43%), bicarbonate and nitrite(49%). Bicarbonate is bound to potassium and nitrate ($r=0.46$ and $r=0.49$ respectively). Silica is bound to both nitrate (47%) and lead ($r=0.47$ and $r=0.49$ respectively).

UNDER PEER REVIEW IN IJAR

Table 8: Correlation matrix for physico-chemical parameters during low-water periods.

	TDS	T,C	Ph	CND	Turb	Ca	Mg	Na	K	Fe	Cl	SO4	NO3	HCO3	Sio2	Zn2,	Pb	PO43,	NO2,
TDS	1,00																		
T,C	0,04	1,00																	
Ph	0,17	-0,19	1,00																

CND	0,60	0,07	0,21	1,00																
Turb	0,16	0,17	0,12	0,07	1,00															
Ca	0,19	0,08	0,19	0,25	-0,15	1,00														
Mg	0,24	-0,44	0,16	0,11	0,33	-0,05	1,00													
Na	-0,24	-0,31	0,15	0,08	-0,21	-0,13	0,02	1,00												
K	0,11	0,42	-0,11	0,32	-0,04	-0,07	-0,03	0,28	1,00											
Fe	-0,19	-0,04	0,31	-0,15	0,38	-0,17	0,23	0,32	-0,18	1,00										
Cl	0,46	0,43	-0,07	0,60	0,26	0,16	-0,05	-0,07	0,18	-0,09	1,00									
SO4	-0,19	-0,24	0,04	0,18	-0,19	-0,39	-0,22	0,45	0,15	0,03	-0,03	1,00								
NO3	0,24	0,43	0,01	0,21	0,36	0,29	-0,18	-0,47	-0,15	-0,07	0,57	-0,19	1,00							
HCO3	-0,27	0,21	0,01	-0,15	-0,09	0,07	-0,19	0,45	0,24	0,20	-0,11	0,14	-0,24	1,00						
Sio2	0,10	0,14	-0,09	0,21	0,14	0,44	0,07	-0,45	-0,37	-0,16	0,26	-0,35	0,55	-0,23	1,00					
Zn2,	0,16	0,12	0,11	0,33	0,21	0,29	-0,01	-0,18	0,10	-0,43	0,25	-0,17	0,30	-0,32	0,08	1,00				
Pb	0,07	-0,13	0,05	0,13	0,15	0,13	0,01	-0,21	-0,18	-0,19	-0,12	-0,13	0,05	0,24	0,50	-0,14	1,00			
PO43,	0,05	0,17	-0,24	0,08	-0,41	0,01	-0,20	0,17	0,47	-0,18	-0,11	0,08	-0,29	0,02	0,05	-0,31	0,08	1,00		
NO2,	-0,14	0,27	-0,21	-0,28	0,07	-0,19	-0,16	-0,24	0,24	-0,26	-0,06	0,18	0,01	0,45	-0,20	-0,08	0,14	-0,06	1,00	

Table 9: Correlation matrix for physico-chemical parameters during high-water periods.

	TDS	T.C	Ph	CND	Turb	Ca	Mg	Na	K	Fe	Cl	SO4	NO3	HCO3	Sio2	Zn2.	Pb	PO43.	NO2.
TDS	1,00																		
T.C	-0,17	1,00																	
Ph	0,17	-0,19	1,00																
CND	0,60	0,04	0,06	1,00															

Turb	0,07	0,26	-0,01	-0,08	1,00														
Ca	0,13	-0,14	0,23	0,07	-0,16	1,00													
Mg	0,39	-0,24	-0,02	-0,06	0,24	-0,15	1,00												
Na	0,22	0,10	-0,03	0,03	-0,08	-0,29	0,44	1,00											
K	0,14	0,16	0,07	0,07	0,49	-0,26	0,13	0,42	1,00										
Fe	0,21	-0,26	0,18	0,07	0,44	-0,05	0,29	-0,28	0,16	1,00									
Cl	0,45	0,44	-0,24	0,58	0,29	0,15	-0,01	-0,10	0,15	-0,12	1,00								
SO4	-0,30	0,09	-0,05	-0,04	-0,07	-0,38	0,14	0,30	0,29	-0,16	-0,04	1,00							
NO3	0,12	0,47	0,07	0,30	0,31	0,33	-0,26	-0,45	-0,19	0,10	0,57	-0,26	1,00						
HCO3	0,07	-0,14	0,28	-0,11	0,06	0,10	-0,29	-0,10	0,46	0,07	-0,11	0,16	-0,23	1,00					
Sio2	0,01	0,14	-0,16	0,07	-0,17	0,32	-0,11	-0,16	-0,46	-0,16	0,17	-0,43	0,47	-0,23	1,00				
Zn2.	-0,18	0,00	0,34	0,14	-0,22	0,27	-0,52	0,16	0,14	-0,53	-0,10	0,14	0,01	0,30	-0,05	1,00			
Pb	0,07	0,05	-0,03	0,10	-0,07	0,16	-0,20	-0,05	-0,21	-0,19	-0,14	-0,13	0,13	0,22	0,43	0,37	1,00		
PO43.	0,19	-0,15	-0,14	0,24	-0,51	0,19	0,04	0,07	-0,18	0,06	-0,05	0,03	-0,28	0,10	-0,04	-0,09	-0,05	1,00	
NO2.	-0,36	0,31	0,04	-0,18	0,01	-0,21	-0,39	-0,16	0,32	-0,23	-0,14	0,17	-0,07	0,49	-0,08	0,32	0,32	-0,23	1,00

IV. 10. Water quality index

The groundwater quality index for the study area ranges from 19.37 to 75.48 at high water (Tab. 10), and from 12.47 to 82.64 at low water (Tab. 11). These values show that the quality of the water analyzed varies from good (25% at high water and 30% at low water) to excellent (75% at high water and 70% at low water).

Table 10: Water quality index for Moundou and surrounding area (December, 2023)

High water period (December 2023)					
works	QWQI	Class	works	QWQI	Class
P1	78,48	Good	F6	47,03	Excellent
P2	39,86	Excellent	F7	45,33	Excellent
P3	21,59	Excellent	F8	46,34	Excellent
P4	33,74	Excellent	F9	40,96	Excellent
P5	34,65	Excellent	F10	68,11	Good
F1	21,12	Excellent	F11	56,94	Good
F2	24,01	Excellent	F12	33,61	Excellent
F3	52,00	Good	F13	23,14	Excellent
F4	19,72	Excellent	F14	58,61	Good
F5	20,70	Excellent	BF	19,37	Excellent

Table 11: Water quality index for Moundou and surrounding area (March, 2024).

Period of low waters (March 2024)					
works	QWQI	Class	works	QWQI	Class
P1	69,03	Good	F6	47,43	Excellent
P2	53,97	Good	F7	48,38	Excellent
P3	21,59	Excellent	F8	35,33	Excellent
P4	19,52	Excellent	F9	42,58	Excellent
P5	23,52	Excellent	F10	84,34	Good
F1	42,76	Excellent	F11	51,24	Good
F2	21,84	Excellent	F12	28,73	Excellent
F3	49,65	Excellent	F13	23,71	Excellent
F4	12,47	Excellent	F14	63,60	Good
F5	14,66	Excellent	BF	82,64	Good

IV.11. Bacteriological parameters

The results of bacteriological analyses (Tab.12, Tab.13 and Tab.14) show that at high and low water levels, groundwater has a dominant concentration of *E. coli*.

Table 12: Variation of bacteria in well water at low and high water levels

Wors	Well	
Low water	Higr water	

	Min.	Max.	Moy.	Ecart.	Min.	Max.	Moy.	Ecart.
E. Coli	53,00	566,00	240,60	212,96	123,00	353,00	272,00	129,20
Coli. Totaux	67,00	270,00	143,20	87,49	70,00	205,00	138,33	67,52
F. Méso.	155,00	200,00	177,60	21,13	164,00	211,00	194,33	26,31
Germes T.	150,00	213,00	179,40	23,06	111,00	200,00	142,67	49,74
Entéro. F	0,00	79,00	32,80	31,54	0,00	15,00	6,67	7,64

Tableau 13:

Variation des bactéries dans les eaux des forages en basses et hautes eaux

Works	Drilling							
period	Low water				High water			
	Min.	Max.	Moy.	Ecart.	Min.	Max.	Moy.	Ecart.
E. Coli	96	543	349,4	185,61	91	400	217,6	147,77
Coli. Totaux	21	200	99	82,43	39	164	99,2	49,62
F. Méso.	70	198	149,8	48,52	66	250	190,6	73,51
Germes T.	57	200	148	55,55	103	200	140	38,68
Entéro. F	0	44	8,8	19,67	0	13	2,6	5,81
Entéro. F	0	44	8,8	19,67	0	13	2,6	5,81

Tableau 14 : variation des bactéries dans l'eau de la borne fontaine

Settings	E. coli	Coli. totaux	F. mésophile aérobie t.	Germe t.	Entéro. F.
Low water	303	261	185	211	23
High water	656	261	190	205	40

V. DISCUSSION AND INTERPRETATION

V.1 Inventory of water production facilities in and around Moundou

. Most of these structures are installed without any prior study and are found in uncleanont un alentours locations, markedsometimes avec by the presence of animalsau on the immediate perimeter. This is due either to: (1) the population's lack of awareness of the danger posed by stagnant water and debris of all kinds around these structures; (2) the siting of these structures in depressions and/or waterways. Raising awareness of the need for sanitation in the surrounding area, and of the location of water catchment structures, would eradicate these notoriously unsanitary problems; (3) the practice of raising livestock without enclosures, so that animals roam around and approach watering points to drink from the water poured along the edges of the structures, and to take advantage of the humidity. The lack ofassainissemnt sanitation around AEPs in urban areasont aussi has been noted by other authors (Djimrabaye,2018 ; Dingamadji, (2019, Kadjangaba *et al.*2023).

V.2. Health surveys

The results of the survey carried out at the Logone provincial health delegation show a resurgence of water-borne diseases such as typhoid fever and dysentery. These diseases are of faecal origin (George and Servais, 2002; Adetunde and Glover, 2011). The causes of disease are attributable to the ingestion of contaminated water, linked to the absence of sanitation facilities. Between 2015 and 2016, the prevalence of these diseases is low (Fig.11), this would be explained by the demographic average during this period. Diarrhoeal diseases peak between 2018-2019, while typhoid fever remains almost constant (Fig.5.a). These episodes coincide with population growth (Fig.11. b), which is likely to exert strong pressure on the facilities that have led to the degradation of the bacteriological quality of water and as a consequence the resurgence of water-borne diseases. After these peaks, prevalences are declining while the population continues to grow, this is attributable to the WASH projects instituted by the Government and its partners in the city of Moundou since 2015 (DEA, 2024). This project has intervened in the supply of drinking water and sanitation through the installation of latrines complying with sanitary standards. The results of these sanitary surveys corroborate those of Ndeko *et al*, (2018), Djimrabaye (2018), Digamadji (2019), Eloge (2015), Jean *et al*, (2013).

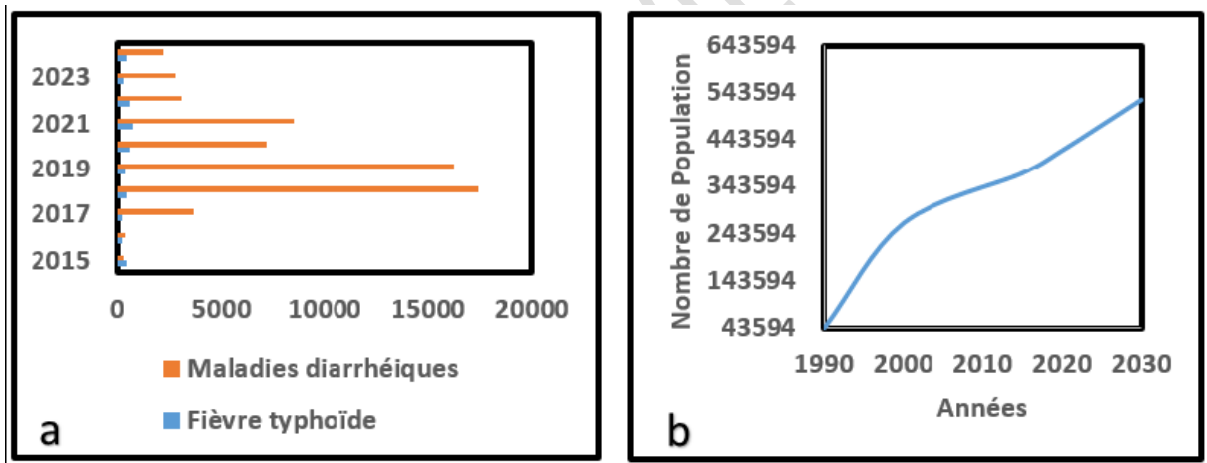


Figure 11 : Disease (a) and population (b) trends.

Sources: (a) Délégation de la santé du Logone Occidental (2024); (b) City Fast (2019).

V. 3 Hydrodynamic parameters

V.3.1. Piezometry (December 2023-March 2024).

Processing of data from piezometric campaigns shows that the difference in static levels between the two periods (issues des deux campagnes : high water and low water) is between 0.44 and 2.1 m (Fig.12). The increase in static level at high water is probably due to groundwater recharge during this period by rainwater infiltration. Whereas on the lowering of the static level during low-water periods is due to the use of groundwater by the population and evapotranspiration.

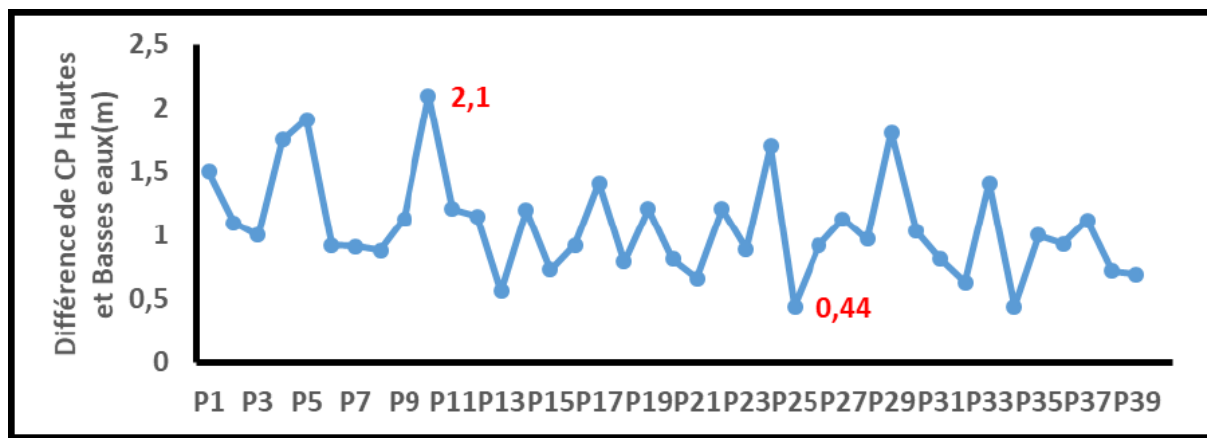


Figure 12: Static level difference between low and high water

The piezometric maps (Cf Fig.4) drawn up from data collected during high-water periods show two (2) domes (in pink, located to the west and north of the study area) and three (3) piezometric depressions (in light blue, located to the south and east of the area), two (major located to the east) and one (1) medium (located to the south). Groundwater flows in two directions depending on the slope of the isopiezies, with water flowing from steep to shallow slopes. It flows from north and west to south and east, concentrating in the piezometric depressions located in this part of the study area. Water flowing north and north-west will certainly flow certainly into a depression located outside the study area beyond Torodjo. According to Castany (1982), domes are groundwater recharge zones, whereas depressions are groundwater discharge zones. For Archambault (1987), piezometric depressions are zones not subject to recharge but exposed to evapotranspiration, while Ngounou (1993) concludes that piezometric depressions are zones associated with evapotranspiration and the passage of the water table in the lower clays. In the study area, recharge zones are located to the west and north, and discharge zones to the west and south. The behaviour of the piezometric level observed in the field shows that in the study area, piezometric depressions are due to: (1) overexploitation of groundwater; (2) a drop or lack of recharge following soil compaction in connection with intense urbanization; (3) overexploitation in connection with demographics. The piezometric slope decreases the closer you get to the watercourses, showing that in addition to direct recharge at the piezometric cones, the depressions receive indirect recharge from the watercourses. In addition, this piezometric map provides us with information on areas suitable for the installation of test pumping and catchment structures for the APE (Alimentation en Eau Potable), i.e. the piezometric depressions located to the south and east (in the Taye district and to the south of the Masdagascar district).

V.4. Physicochemical parameters and bacteriological parameters

V.4.1. Variation in physico-chemical parameters

V.4.1.1. physical parameters

The average values of the physical parameters recorded in tables (1,2,3,4,5,6 and 7) show that the TDS, conductivity and turbidity of the low-water boreholes and the hydrant comply with the WHO standard (2017). On the other hand, the average values for temperature, pH and turbidity for wells and boreholes in high water do not comply with the WHO standard (2017) for water

intended for human consumption. What are these average values, and what is the standard value WHO(2017).

- STD

TDS (Total Dissolved Solids) measures the total concentration of dissolved solids in a solution. This includescompris minerals, salts, metals and other substances present in the water. The TDS values obtained in the present study areleur ensemble inférieurs lower than the potability standard set by the WHO (2017). This is due to the nature of the sandy aquifer. The TDS values obtained in this study are in the same class as those determined by Allarassem *et al*, (2023), Digamnadj (2019). These authors carried out their study in the same locality

- Temperatures

The map (Fig.13.) of groundwater temperature distribution in the study area shows a decrease in temperature as you move towards the watercourses. Moreover, average temperature values are close to the average atmospheric temperature in the study area (29°C). This can be explained by (1) the influence of ambient temperature on shallow groundwater, (2) the effect of the geothermal gradient on deep water (located to the west and northeast of the study area), (3) the influence of the Logone River through infiltration during low-water periods for water located near this river. High groundwater temperatures are conducive to the development of environmental micro-organisms (Asaï *et al*.2023). These high groundwater temperature values have also been highlighted by other authors working in similar environments, including Kadjangaba (2023), Tomasbé (2015) and Dingamadji, (2019), Djimrabaye (2018), Kamena (2021).

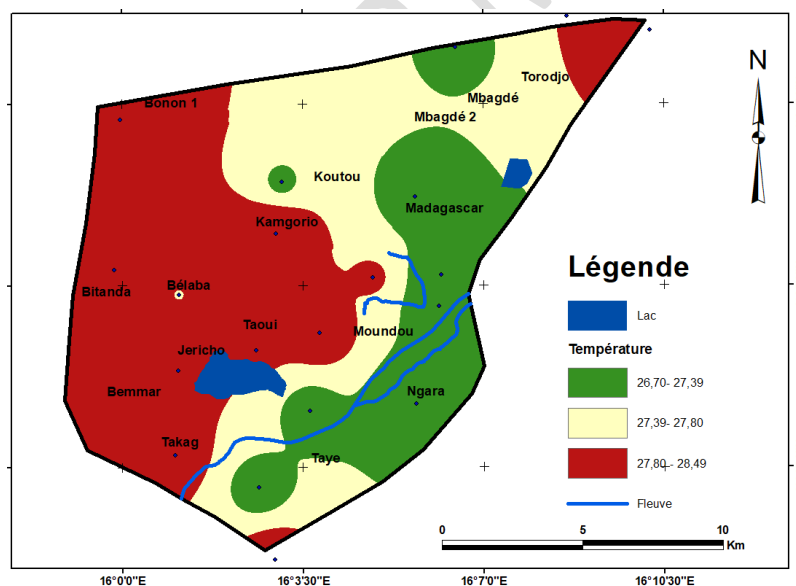


Figure 13: Groundwater temperature distribution map

- Turbidity

Turbidity provides information on the presence of suspended matter, notably clays, silts, fibrous particles, colloidal organic matter, plankton and microspic organisms (Frahtia and Nezzar,2016). The distribution map of- turbidities (Fig.14) shows that the highest values are observed at Ngara

and Kamgorio (to the east and center), where groundwater is mainly exploited à l'aide in wells. Generally speaking, well water in the study area is more turbid than borehole water. This may be due to the exposure of the wells to aerosols, since in most cases they have no curbstones and/or closures, on the one hand, and the use of pushers lying on the ground, on the other. Turbidity is also associated with erosion of the well walls, most of which are not stabilized by a support (brick construction, nozzles or shafts), or with the failure

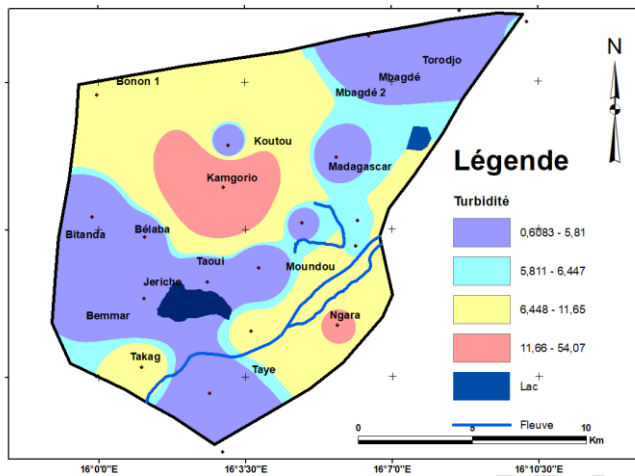


Figure 14: Groundwater turbidity distribution map

• pH

The spatiotemporal distribution of pH values (Fig.15) shows that the most acidic waters are found to the west (in the Bonon, Bitanda, Bemmar and Jericho districts) qui coincide , coinciding with the piezometric cones (see Fig.4), to the south (Taye district), to the east and to the northeast. Average pH values show that groundwater is acidic. These acidic pH values could be linked to: (1) la the infiltration of CO₂-rich rainwater; (2) the dissolution and infiltration of humic acids resulting from the decomposition of organic matter, particularly in the most acidic waters located in districts with high levels of agro-pastoral activity; (3) the sandy nature of the geological formation, confirming the findings of(Tamonkem *et al.* (2024), comme le cas du secteur d'étude . This low pH could bedue due to high levels of free CO₂, themselves linked to the presence of microorganisms such as fungi and coliforms (Tamonkem *et al.*2024). For the WHO (2017),la faible the lowPH pH of a water has no direct impact on consumers but is rather an indicator of the presence of micro-organisms. Such water must be treated to eliminate microbes before consumption.

Several authors have reported on the acidic nature of water in continental aquifersst andsabloneux sandy. These include Tchadanaye and Tarkodjiel (2009); Tomasbé (2015); Dingamadji, (2019); Kadjangaba *et al.*, (2023); Kengni *et al.*, (2012); Kamena (2021); Ngouala *et al.*, (2020); Germain *et al.* (2019); Tamonkem *et al.*, (2024); Photo *et al.*, (2022); Germain *et al.*, (2019). On the other hand, the work of Allarasse *et al.* (2023), carried out in a region adjacent to the study area, revealed basic groundwater. This difference lies in the lithological nature of the aquifers.

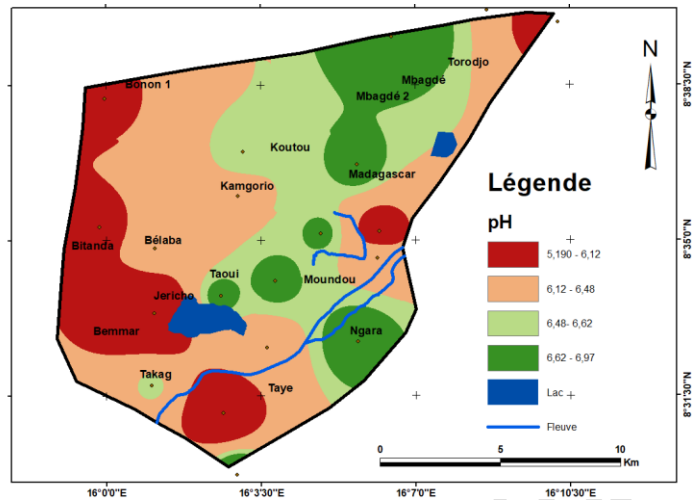


Figure 16: Groundwater pH distribution map

- Conductivity

Groundwater conductivity in the study area is low to medium, due to the nature of the aquifer, which is rich in sandstone and sand. In addition, the lowest values (Fig. 16) can be observed in the vicinity of watercourses, demonstrating the influence of surface water on groundwater conductivity through infiltration and dilution. For Tamonkem *et al*, (2024), the low conductivity values suggest a low rate of solubilization or exchange between groundwater and the surrounding aquifer materials. These waters fit into the group of those determined by other authors (Djoret, 2000; Kengni *et al*. 2012; Ngouala *et al*. 2020; Tomasbé, 2015; Mardochée, 2019, Allarasse *et al*. 2023).

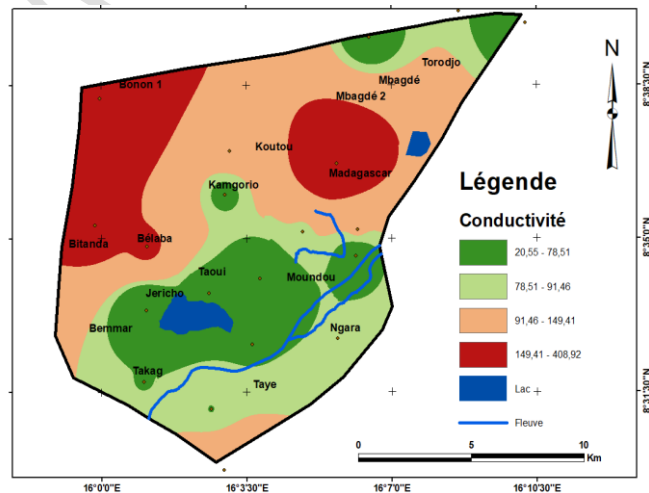


Figure 16: Groundwater pH distribution map

V.4.1.2. Chemical parameters

Changes in the average values of chemical parameters (see Fig. 5.a, Fig. 7 and Fig. 9) show that, apart from potassium, silica, phosphate and nitrite, the values of the other parameters comply with the potability standard set by the WHO (2017).

- Potassium

Potassium distribution maps for low and high water levels (Fig. 17) show that the highest concentrationsd'étend are recorded in peripheral areas with high agricultural and grazing activity. For White *et al* (1999), potassium is mainly released by the weathering of alkali feldspars and especially biotite, while for Guy (2012), potassium in groundwater is explained by the exchange of bases with clays. The high potassium levels in the water in the study area are explained by anthropogenic action, in particular the leaching and infiltration of chemical fertilizers named NPK, massively used in market gardening and other food crops in the outlying districts. The work of Kadjangaba *et al*(2023) and Tomasbé (2015) also noted high levels of potassium in the area's groundwater. According to Léas (2024), excess potassium can disrupt the functioning of thecoeur heart, causing heart rhythm disorders and even cardiac arrest.

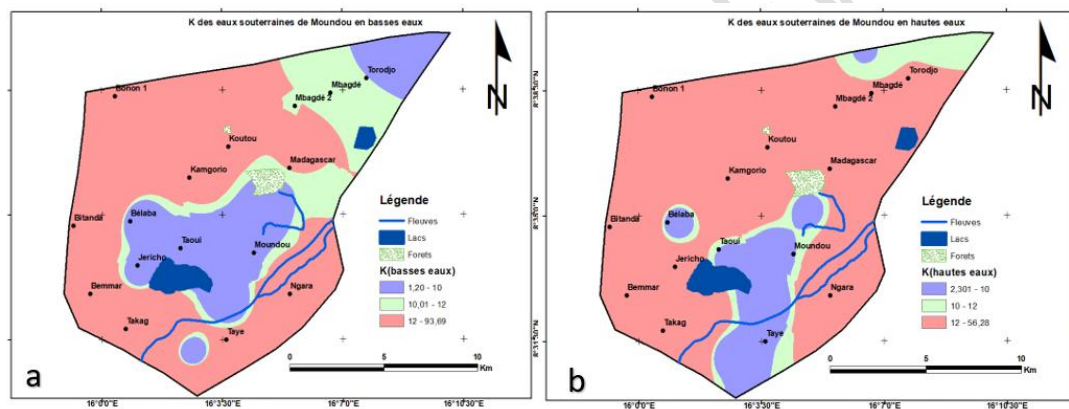


Figure 17: Potassium concentration in low (a) and high (b) water.

- Silica

Analysis of the silica content map (Fig. 18) for high and low water levels shows that there are only three small pockets where concentrations comply with the WHO standard (2017). The silica excess can be explained by: (1) the predominantly sandy nature of the geological formations of the Continental Terminal; (2) the phenomenon of monosialitization and bisialitization; (3) the exposure of wells to aerosols most often laden with weathered materials. Indeed, the works of (Paul *et al.* 1969, Camille, 2015, Ngouala *et al.*2020, Hamid, 2012) have noted the excess of silica in groundwater. For the 2(nd) and 3(rd) authors, silica enrichment in water is linked to base exchange between water and the surrounding terrain, and the second author characterizes silica richness as evidence of a long residence of water in geological formations, while for the third author, the high silica content in groundwater finds its explanation in the alteration of

plagioclases, notably that of albite. According to Eblin *et al*, (2014), high silica levels in drinking water, as is the case in the study area, could result in lung pathologies.

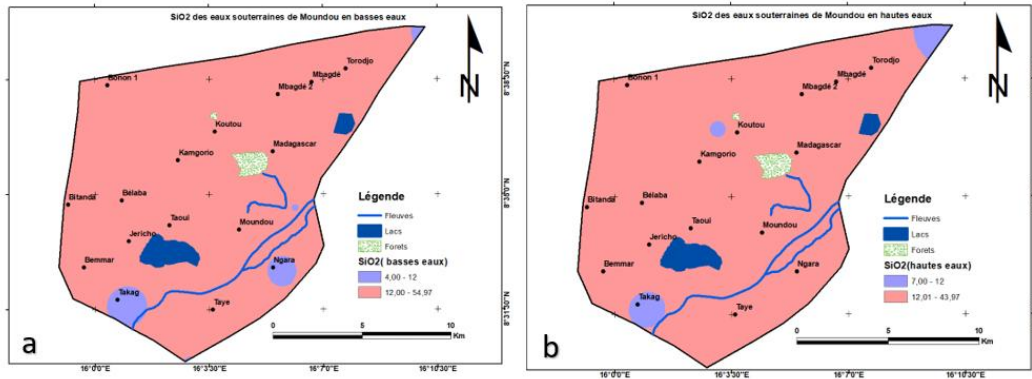


Figure 18: Silica concentration in low (a) and high(b) water (March,2024).

• Nitrate

Nitrate concentrations in both low and high waters are in line with the WHO (2017) recommendation for water intended for human consumption, but values above 10mg/l still suggest anthropogenic involvement. According to Madison and Brunett (1985), a NO_3^- concentration between (0.21-3mg/l suggests possible anthropogenic action and 3.1-10 mg/l indicates a very clear influence of anthropogenic action.

Maps of nitrate distribution show low to average values in the southern part of the study area around the Logone River, which is probably linked to dilution by surface water (Fig.19). Furthermore, the high nitrate values ($> 3\text{mg/l}$) in groundwater in and around Moundou could be linked to: (1) the leaching and infiltration of chemical fertilizers utilisation utilisés dans les (2023), resulting from agricultural activities; (2) the use of full-bottom latrines, which allows communication between the water table and human waste, especially during high-water periods; (3) decomposition of organic matter of animal and plant origin; (4) lessivage leaching and infiltration of animal dejecta. Les auteurs, Nesma et al, (2022); Djoret (2000), Kadjangaba *et al*. Mardochée (2019) and Tomasbé (2015) have reported high nitrate values in groundwater in sedimentary and urban environments. These authors index anthropogenic factors as the origin of nitrate in groundwater. High nitrate levels can cause methemoglobinemia in infants and carcinogenic diseases in adults (Johnson, 2019).

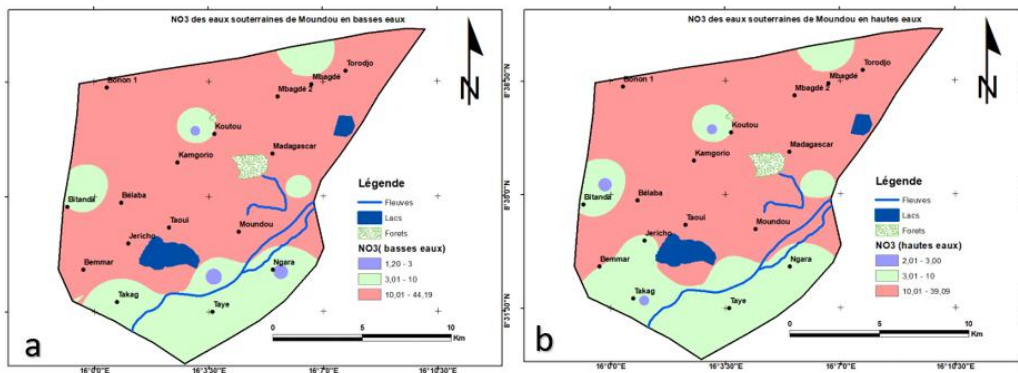


Figure 19: Nitrate concentration in low(a) and high(b) water.

- **Nitrite (Fig.20)**

The distribution of nitrites in groundwater shows that in both high and low waterleur their valueallent varies respectively 28 and 23 times higher than that set by the WHO (2017). Moreover, the presence of nitrites in water suggests deterioration in quality throughprésence microbes (Vincent, 2019). There are four small pockets (in grey to the north, south, east and west) with concentrations in line with the potability standard. Thismarque supports the low level of anthropic action at the points concerned, or the discharge of water from these points towards the piezometric depressions, as these points coincide with the piezometric domes. In this locality, nitrites would mainly come from anthropic activities (incomplete oxidation of solid or liquid waste or chemical fertilizers used for soil fertilization by man) as also attested by the work of Kadjangaba *et al.*(2023) and, Tomasbé (2015) .

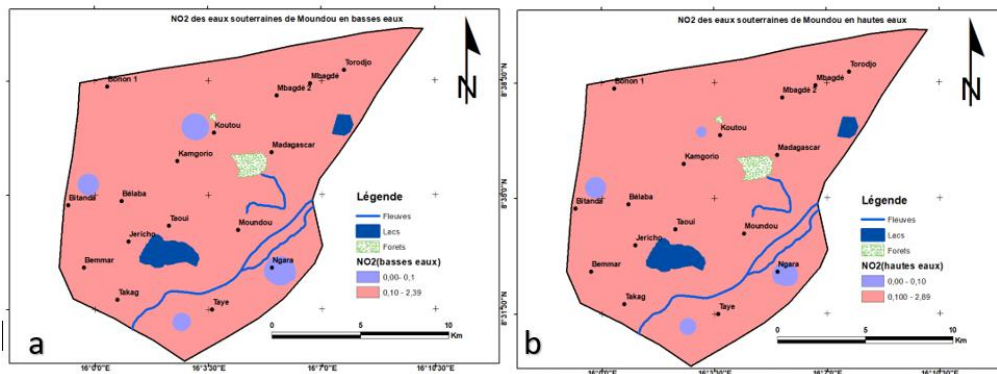


Figure 20: Nitrite concentration in low (a) and high (b) water.

Phosphate

Phosphate distribution maps (Fig.21) for groundwater in and around Moundou show that levels are 99% higher than the standard value set by the WHO (2017) for water intended for human consumption. In both high and low waters, the highest values are due to: (1) the use of phosphate-rich detergents, (2) the infiltration of phosphates from human excrement, and (3) the high values obtained in the outlying districts are linked to agro-pastoral activities (infiltration of chemical fertilizers). These waters fall into the class of those studied by Kundu *et al.* (2015), Ngouala *et al.*2020), who reported high concentrations of phosphates in groundwater and concluded that they originate mainly from industrial and domestic discharges (human excreta, detergents, laundry detergents).

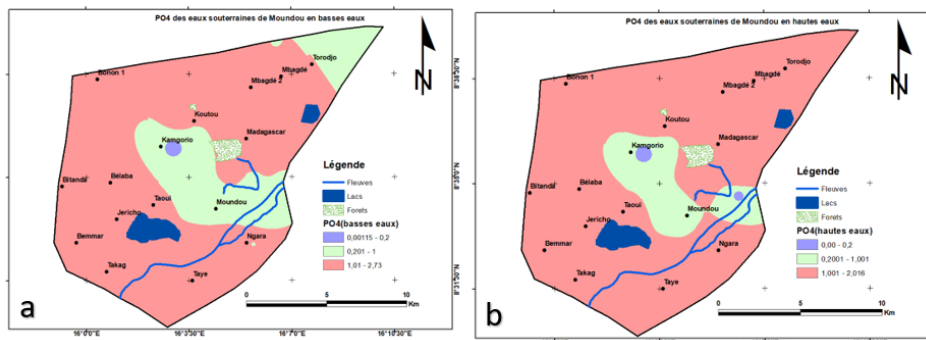


Figure 21: Phosphate concentration in low (a) and high (b) water.

- **Iron**

The iron distribution map (Fig.22), highlights four pockets (Fig.22.a) in the lowlands with levels in compliance with the WHO potability standard (2017). In high water (Fig.22. b), the waters to the west meet the WHO potability standard (2017), while those to the east and at the periphery of the watercourses have a concentration above the WHO standard (2017). This is linked to the drainage of dissolved iron into watercourses, which in turn impacts the quality of groundwater in their vicinity. Iron concentration values for boreholes are slightly above the standard at both high and low water levels. The high iron content of these waters is thought to be due to: (1) oxidation of water-operating equipment (in the case of human-driven pumps), (2) degradation of the drums used to stabilize the walls of latrines and/or wells, or the burial of certain metals mixed with the garbage used to backfill depressions, (3) leaching from iron-rich geological formations such as laterite/bauxite. With such high iron contents, the waters of this study area are among those identified by Germain *et al.* (2019), Kadjangaba *et al.* (2023) and Djimrabaye (2018). These studies, have also reported the presence of iron at high.

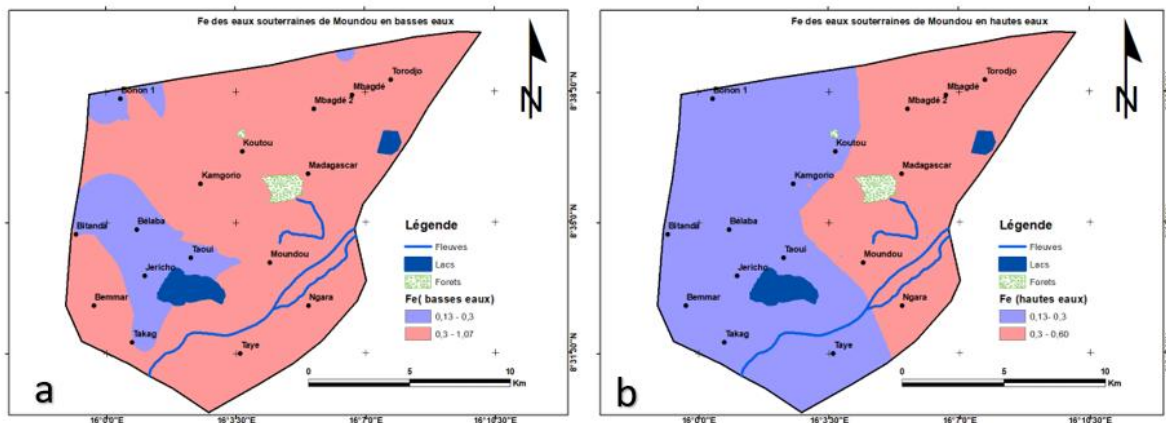


Figure 22: Iron concentration in low (a) and high(b) water (March,2024).

V.5. Hydrochemical facies

The results of water analysis show that 90% of low-water waters belong to the bicarbonate calcic and magnesian facies (low and high waters), 50% (25% low water and 25% high water) of waters belong to the chloride and sulfate calcic and magnesian facies, 10% in low water and 20% in high water belong to the carbonate sodium and potassium facies, while the chloride sodium and potassium or sulfate sodium facies occupies 15% of waters in low water and 15% in high water respectively.

Calcium-magnesium bicarbonate facies characterizes the immature waters of sedimentary aquifers (Hamit, 2012) and generally represents poorly mineralized waters with conductivities below 1000 $\mu\text{S}/\text{cm}$ (El Alaoui, 2010). The predominance of this facies in the waters of the study area is probably linked to: (1) the dissolution of atmospheric CO_2 , followed by percolation of

these waters to the water table, (2) the alteration of dolomite or feldspars such as anorthite to kaolinite.

The presence of sodic and potassic carbonate facies on the one hand, and sodic and potassic chloride facies and calcic chloride facies on the other, is explained by the phenomenon of base exchange between the water and the host rock. Calcium chloride facies are alluvial in origin (Seghir, 2014). The chemical facies of the waters in the present study align with the class of facies determined by Djoret (2000), Kadja (2007), Hamit(2012). Tomasbé (2015), Mardochée (2019) under an environment similar to the one studied.

V.6. PCA

V.6.1. Factor analysis

Analysis of 20 individuals and 19 variables (Fig.4.19) shows that, in both low and high water conditions, factors 1 and 2 reflect both anthropogenic and natural mineralization (water-rock interaction). This is because we can observe elements likely to be of anthropogenic origin (phosphate, nitrite, lead, iron, nitrate) and elements of natural origin (bicarbonate, sodium, calcium, potassium, etc.). This shows the diversification of groundwater mineralization in Mondou and the surrounding area.

V.6.1. Correlation

The major correlations between conductivity, STDs and chloride (Cf. Tab.8 and Tab.9) show that in the study area, these parameters are linked in both low and high water.

Moreover, the link between chloride and nitrate in both high and low water suggests a common origin for these elements, which is certainly anthropogenic. The correlation between these parameters was also highlighted by Ngouala (2020), Djigamadji (2019) and Djimrabaye (2018). On the other hand, parameters with a correlation coefficient close to zero (such as; TDS-temperature, Turbidity-temperature) have no link. Those with negative correlation coefficients (such as TDS-sulfate, TDS-bicarbonate) are antagonistic, i.e. when the value of one increases, the value of the other decreases, and vice versa.

V.7. Groundwater quality index for Moundou and surrounding area

Groundwater quality indices show that, overall, the quality of groundwater in and around Moundou, in relation to the sampling point, ranges from good to excellent. Although the concentration of certain chemical elements (phosphate, nitrite, potassium, iron and silica) and physical elements (temperature, turbidity and pH) are non-compliant, this has less impact on the physico-chemical quality of Moundou groundwater. These results are not in line with those of Kadjangaba *et al* (2023), who found that, in addition to the classes obtained in this study, the water was classified as very poor to non-drinkable. This can be explained either by the difference in sampling sites or by the parameters chosen for calculating the index. Ces eaux salignent donc dans le groupe de celle déterminées par Tamonkem *et al.*, (2024).

V.7. Origin of water mineralization

V.7. 1 The Gibbs diagram

The Gibbs diagram shows the evolution of total water mineralization as a function of the ratio $(Na+K) / (Na+K+Ca)$. This diagram makes it possible to distinguish between waters whose mineralization is controlled by evaporation and waters whose mineralization is due to the

influence of water-rock interaction (WRI) or anthropogenic processes. The positioning of the waters in the study area in this diagram at low water shows their positioning in three domains, while at high water they are positioned in two domains.

✓ Low water (30) (Fig.23.a)

The water in the boreholes (F13, F12, F6, F3 and F8) falls within the sphere of influence of both the water-rock interaction process and the evaporation phenomenon.

Water from wells (P3, P5 and P2) falls within the evaporation sphere of influence. Water from boreholes (F5, F14, F10, F9, F11, F1, F7, F2, F4), wells (P4, P1) and the fountain hydrant (BF) belong to the anthropogenic sphere of influence.

✓ High water (Fig.23.b)

Seventy-five percent (75%) of the water belongs to the area of influence of evaporation, i.e. water from boreholes (F13, F12, F3, F8, F6, F14, F1, F10, F5, F4, F2), wells (P2, P3, P5) and the fountain hydrant (BF) belong to the area of influence of evaporation ;

Twenty-five percent (25%) of the water is under anthropogenic influence, notably water from boreholes (F11, F1, F9) and wells (P4 and P1). The control of water mineralization by evaporation is due to: (1) the shallow depth of the water; (2) the rise in temperature at both high and low water levels; (3) the influence of streams in contact with the water table; (4) the hydrolysis of evaporites such as halite, gypsum and anhydrite, as reported in the study area by Schneider (2001). The influence of anthropogenic action on water is linked to: (1) the proximity of structures to possible sources of pollution such as garbage heaps, dump holes, latrine emptying and the presence of animals; (2) unsanitary conditions around these structures (Cf. Fig.19.a, b and c); (3) infiltration of household and industrial wastewater; (4) infiltration of

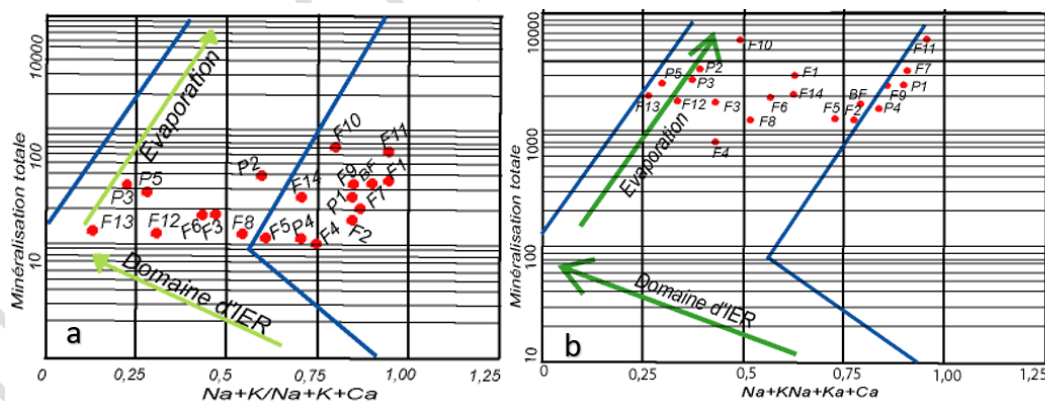


Figure 23: Projection of low (a) and high (b) water in the Gibbs diagram (1970)

V.7.2. State of equilibrium of analyzed waters

The Korjinski diagram (Fig.24) shows that the waters analyzed are in equilibrium in order of abundance with secondary minerals such as montmorillonite ($[(\text{Si}(3) \text{ (.) (67)}\text{Al}(0) \text{ (.) (33)})\text{O}(1) \text{ (0)}\text{Al}(\text{OH})_2\text{Ca}_{2+} 0.167]$), kaolinite ($[\text{Al}_2\text{Si}(2) \text{O}(5) (\text{OH}) (4)]$), albite ($\text{NaAlSi}_3\text{O}_8$), dolomite ($\text{CaMg} [\text{CO}(3)]_2$) and microcline (KAlSi_3O_8). One of the alteration processes influencing the

mineralization of water in and around Moundou is therefore hydrolysis through allitization (total elimination of base cations and silica, giving rise to type 1/1 clays, as in the case of kaolinite) and bisiallitization (partial leaching of silica and base minerals. K^+ and Na^+ giving rise to type 2/1 clays; this is the case of montmorillonite) and dolomitization (alteration of limestone by magnesium-rich water).

magnésium).

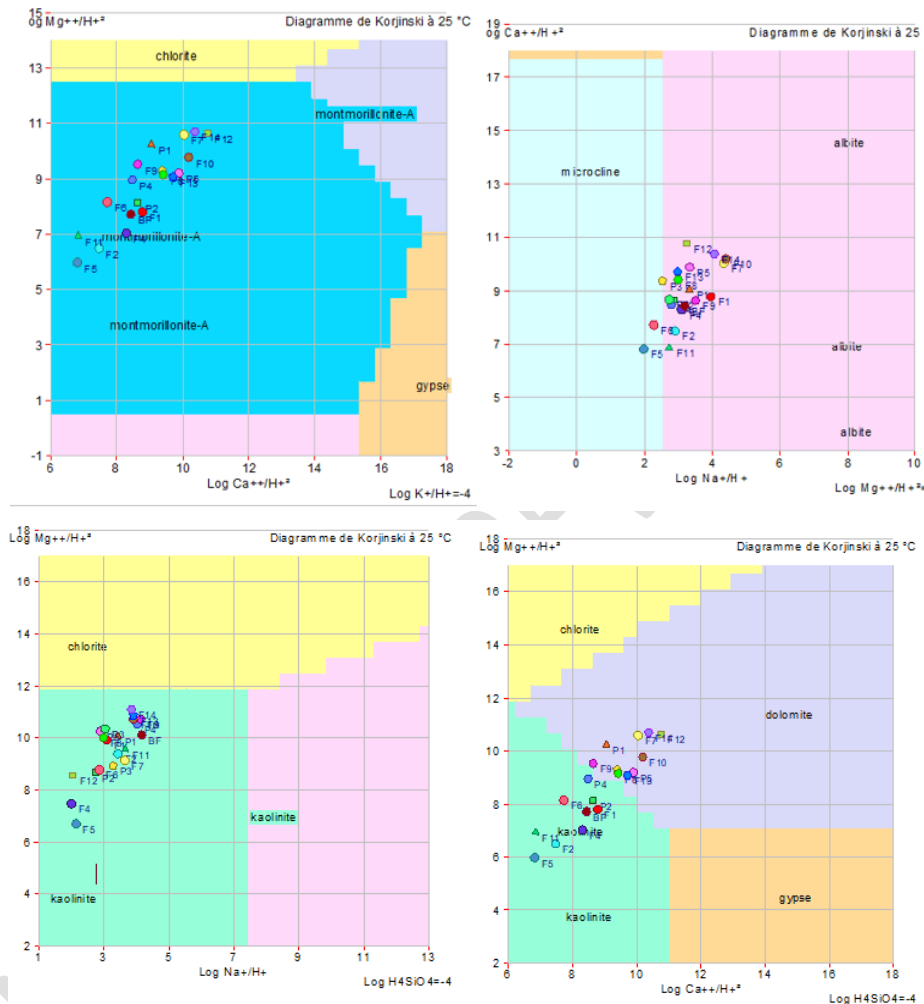


Figure 24: Korjinski diagramdonnant les of the main minerals in equilibrium with the water analyzed .

General conclusion

The aim of the study was to determine the quality of groundwater in and around Moundou. Les descentes sur le terrain The various approaches revealed that the most commonly used water supply structures in the study area are boreholes equipped with human-powered pumps and traditional wells. These facilities, located inont a dirty environmentavec la présence d'ouvrages lack sanitationindividuelle et des and mix with household waste dumps. The piezometric mapsmontrent que have also identifiedles groundwater recharge zones locatede nt to the west and

north of the study area, and landfill zones to the south and east of the study area, highlighting the flow of groundwater towards the Logone River. The physico-chemical characterization of the sampled waters highlighted the acidity ($5.09 < \text{pH} < 6.98$) and low to medium mineralization ($15.60 \mu\text{S}/\text{cm} < \text{C.E} < 409 \mu\text{S}/\text{cm}$) of the groundwater in and around Moundou. This is related to the sandy Continental Terminal aquifer. These waters also have a turbid character in relation to both natural and anthropogenic activities. The temperature of all the water analyzed is above the WHO standard (2017).

Chemical parameters show that nitrite, phosphate, silica and iron values in some waters exceed the WHO standard (2017). The dominant chemical facies is calcium-magnesium bicarbonate (low and high water). This is followed by the chloride and sulfate calcium-magnesium facies. The GWQI shows that groundwater in the study area is of excellent to good quality. From a bacteriological point of view, both low and high water levels in the study area were contaminated by microorganisms, with levels above the WHO (2017) standard values for drinking water. The presence of these bacteria is proof of contamination of fecal origin and of the non-drinkability of this water, whatever the number of germs, even 1 in 100 ml of sampled water (OMS, 2006 ; Mehanned *et al*, 2014 ; Sila, 2019) . This faecal contamination is linked to the widespread use of full-flush latrines. The presence of *E. coli*. The presence of *E. coli*. is indicated by faecal matter.

Bibliography

- Adesakin A. T, Oyewale T. A, Bayero U, Mohammed A. N, Aduwo I. A, Zubeidat P.A, Dalhata N. A, Balkisu I. B., (2020).** Assessment of bacteriological quality and physico-chemical parameters of domestic water sources in Samaru community, Zaria, Northwest Nigeria, Elsevier, Heliyon (6) e04773, 13 p.
- Adetunde, L.A., Glover, R.L.K. (2011).** Evaluation of bacteriological quality of drinking water used by selected secondary schools in Navrongo in Kassena- Nankana district of upper east region of Ghana. Prime J. Microbiol. Res. 1, 47–51.
- Archambault J., (1987).** Réflexion sur l'alimentation et l'évapotranspiration des nappes phréatiques en Afrique Subsahari
- Asaï A. G. A., Déhalé D. A., Jean S., Ingrid C. G., (2023).** Qualité physico-chimique et bactériologique des eaux souterraines dans l'arrondissement de Zinvié au Bénin . RASS. *Pensées Genre. Penser Autrement*. VOL 3, No 2.
- Bello, O.O., Osho, A., Bankole, S.A., Bello, T.K., (2013).** Bacteriological and physicochemical analyzes of borehole and well water sources in ijebu-ode, southwestern Nigeria. Journal of Pharmaceutical and Biological Research 8 (2), 18 25.
- Bouchemal F. & Achour S., (2015).** Qualité physico-chimique et paramètres de pollution des eaux souterraines de la région de BISKRA. Larhyss Journal, 22 : 197-212.
- BRGM (1992).** Evaluation Hydrologique de l'Afrique Sub-Saharienne Pays de l'Afrique de l'Ouest. Rapport de pays : Tchad, 501p.
- BRGM (1987).** Actualisation des connaissances sur les ressources en eau souterraine de la république du Tchad : présentation générale et bibliographique. *Synthèse des données géologiques et carte 1/500 000*, 44p.

- Camille B., (2015) :** Bilan et dynamique des interactions rivières-lac(s)-aquifères dans le bassin hydrologique du lac Tchad. *Thèse pour l'obtention du grade de Docteur*, Université d'Aix-Marseille, 295p.
- Castany G., (1982) :** Principes et méthodes de l'hydrogéologie. *Collection Dunod*, Université de paris, 2^e édition, 236p
- Diallo T. (2017).** Bacteriological quality of drinking water; Doctoral thesis in Pharmacy, Faculty of Medecine of pharmacy and Odontostomatology, University of Bamako, 32P.
- Dingamadji M., (2019). Etude de la vulnérabilité a la pollution des eaux souterraines dans le centre urbain de Moundou. *Mémoire de master*. Université de Dschang, 62p.
- Djimarabaye M., (2018).** Etude de la vulnérabilité à la pollution des eaux souterraines et santé de la population du quartier Toukra dans le 9^{ème} Arrondissement la ville de N'djaména (Tchad). *Mémoire de master en Science de la terre*, Université de Dschang, 98p.
- Djoret D., (2000).** Etude de la recharge de la Nappe du Chari Baguirmi (Tchad) par les méthodes chimiques et isotopiques. *Thèse de doctorat Ph. D*, Université d'Avignon et des Pays de Vaucluse, 186p.
- Dovonou F, Aina M, Boukari M et Alassane A., (2011).** Pollution physico-chimique et bactériologique d'un écosystème aquatique et ses risques écotoxicologiques : cas du lac Nokoue au Sud Benin ; Int. J. Biol. Chem. Sci. 5(4) : 1590-1602.
- Eblin S. S. G., Sombo A., Aka N., Kambiré O., (2014).** Hydrochimie des eaux souterraines de la région d'Adiaké (sud- est Côte d'Ivoire). *Larhy J.*, 17 : 193-214. DOI : 0.4236/Nr.2015.611050.
- El Alaoui, E. A. H., Hajhouji Y., (2010).** Hydrochimie et qualité des eaux de surfaces et souterraines du Haouz. *Mémoire de de licence en science de la Terre*, Université de Marrakech(Maroc), 47p.
- Esharegoma, O.S., Awujo, N.C., Jonathan, I., Nkonye-Asua, I.P., (2018).** Microbiological and physicochemical analysis of Orogodo River, agbor, delta state, Nigeria. *International Journal of Ecological Science and Environmental Engineering* 5 (2), 34–42.
- Fehdi C., Boudoukha A., Rouabhia A., Salameh E., (2009).** Caractérisation hydrogéochimique des eaux souterraines du complexe aquifère Morsott-Laouinet (Région Nord de Tébessa, Sud-Est algérien). *Afrique Science*, 5(2) : 217 – 231.
- Ferguson G., McIntosh J.C., Warr O., Sherwood Lollar B., Ballentine C.J., Famiglietti J.S., Kim J-H., Michalski J.R., Mustard J.F., Tarnasad J. et MacDonnell J.J., (2021).** « Crustal groundwater volumes greater than previously thought ». *Geophysical Research Letters*, vol. 48, no 16.
- Hamit A., Isseini M., Abdraman M., Brahim H., Moumtaz R., (2013).** Le système aquifère de Chari Baguirmi (République du Tchad). Caractérisation hydrochimique du système en vue de sa gestion durable. *Revue Scientifique du Tchad* : 1017 – 2769, 9 p.
- Garin H., (1979).** Programme d'hydraulique Villageoise dans les Préfectures de la Tandjilé

- du Logone occidental et du Logone Oriental suivie technique et contrôle de travaux de forage, 131p.
- Germain K. N., Jules M. M., Narcisse K. A., Aristide G. D., Lanciné D. G., (2019).** Caractérisation hydrogéochimique des eaux souterraines du bassin versant de la Baya, Est Côte d'Ivoire. *Int. J. Biol. Chem. Sci.* 13(1) : 574-585.
- George I., Servais P., (2002).** Sources et dynamique des coliformes dans le bassin de la Seine. *National de la Recherche Scientifique, Paris, France*, 46 p.
- Gnazou M.D.T., Assogba K., Sabi B.E., Bawa L.M., (2015). Qualité physico-chimique et bactériologique des eaux utilisées dans les écoles de la préfecture de Zio (Togo). *Int. J. Biol. Sci.* 9(1): 504-516.
- Guy Moukandi N'kaya (2012).** Etude Hydrogéologique, Hydrochimique in situ et Modélisation Hydrodynamique du Système Aquifère du Bassin Sédimentaire Côtier de la Région de Pointe-Noire. Hydrologie. Université Marien N'Gouabi (Congo), Thèse de doctorat, 142p
- Hamit A., (2012).** Étude du fonctionnement hydrogéochimique du système aquifère du Chari Baguirmi (République du Tchad). *Thèse de doctorat Ph. D*, Université de Poitiers 324p
- Hamit A., Isseini M., Abdraman M., Brahim H., Moumtaz R., (2013).** Le système aquifère de Chari Baguirmi (République du Tchad). Caractérisation hydrochimique du système en vue de sa gestion durable. *Revue Scientifique du Tchad* : 1017 – 2769, 9 p.
- Haslay C. & Leclerc, H. (1993).** Microbiologie des eaux d'alimentation. Technique et documentation, lavoisier, 1ère éd., Paris, France, 495 p.
- Issa, H., (2007).** Influence de la lithologie sur les eaux des nappes de N'djamena. Mémoire de Licence professionnelle en hydrogéologie. Institut Universitaire de Mongo-Tchad, 63p.
- INSEED (2015).** Enquête Démographique et de Santé et à Indicateurs Multiples au Tchad (EDS-MICS). 655p
- INSEED (2009).** Second General Census of Population and Housing in Chad. Pages 89. 24.
- Kadjangaba E., (2007).** Etude hydrochimique et isotopique du système zone non saturée de la nappe dans la zone urbaine de N'Djamena : impact de la pollution. *Thèse de doctorat Ph. D, Université d'Avignon et des Pays de Vaucluse*, 206p.
- Kadjangaba E., Guindja B., Bande F., Bongo D., (2023). Etude de la qualité des eaux souterraines et de leur aptitude à la consommation : cas de la ville de Moundou (sud-ouest du Tchad). *American Journal of Innovative Research and Applied Sciences. ISSN 2429-5396*, 10p.
- Kamena M., (2021).** Elaboration d'un modèle de protection des eaux souterraines en zone de socle : cas des aquifères fissurés du bassin versant de la Lobo à Nibéhibé (Centre-Ouest de la Côte d'Ivoire). *Thèse de doctorat, l'Université Jean LOROUGNON GUEDE*, 194p.
- Kamnaye M., (2013).** Etude de la vulnérabilité des nappes libres à la pollution dans le bassin du Lac Tchad : cas de Walia à Ndjamen (Sud-Ouest du Tchad). *Mémoire de master en sciences de la terre, Université de Dschang*. 78p.

- Kengni L., Tematio P., Filali K. H., Tepoule. J. N., Tsafack. E. I., Mboumi. T. L., Mounier S., (2012).** Pollution des eaux superficielles et des nappes en milieu urbain : cas de la zone industrielle de Douala-Bassa (Cameroun). *Int. J. Biol. Chem. Sci.* 6(4): 1838-1853.
- Kundu S., Vassanda M., Rajendiran S., Ajay R., Subba R. A., (2015).** Phosphates hates from detergents a eutrophysation of surface *water ecosystem in India*. Vol.108 n°7 : 1320-1325.
- Léa Zubiria (2024).** Eau riche en potassium : liste, bienfaits, dangers. Disponible sur <https://www.passeportsante.net/fr/Nutrition>. (Consulté le 30/05/2025).
- Madisson, R. J., & Brunett, J. D. (1985).** *Overview of the Occurrences of Nitrate in Groundwater of the United States* (pp. 93-105). US Geological Survey, Water Supply Paper 2275
- Mahamat S. A.M., Maoudombaye T., Abdelsalam T., Ndoumtamia A.G., Loukhman B., (2015).** Évaluation de la qualité physico-chimique des eaux d'adduction publique de la Société Tchadienne des Eaux à N'Djamena au Tchad. *Journal of Applied Biosciences*, 95:8973 – 8980.
- Margat J, (2019).** Exploitation and use of groundwater in the world. Pages 52. 20.
- Niambele D, Diarra O, Bagayoko M.W, Samake S, Samake F, Babana, A.H.; (2020)** E valuation of the Bacteriological Quality of the Drilling Water Analyzed at the National Health Laboratory during the First Half of 2019; International Journal of Science and Research (IJSR) ISSN: 2319-7064, 392-395.
- MEEP(2019).** Contamination fécale des nappes phréatiques, 15p.
- Ngouala M. M., Mbilou U. G., Koussoubé Y., (2020) :** Hydrochimie des eaux souterraines du bassin versant de la loua au sud de Brazzaville, Congo. *American Journal of Innovative Research and Applied Sciences*.ISSN 2429-5396
- Ngounou N. B. (1993).** Hydrogéologie d'aquifères complexes en zone semi-aride. Les aquifères quaternaires du Grand Yaéré (Nord Cameroun). *Thèse de Doctorat*, Univ. de
- Okoli, E.N., (2012)** Evaluation of the bacteriological and physicochemical quality of water supplies in Nsukka, Southeast, Nigeria. *Afr. J. Biotechnol.* 11(48), 10868–10873. Grenoble I, 357 p
- OMS. (2017).** Directives pour l'eau potable: quatrième édition incorporant le premier addenda. Geneva: Organisation Mondiale de la Santé. Licence: CC BY-NC-SA 3.0 IGO, 631p.
- OMS & UNICEF, (2018).** Progrès en matière d'assainissement et d'eau potable ; Rapport. 98 p.
- Ounoki S et Achour S (2014).** Evaluation de la qualité physicochimique et bactériologique des eaux usées brutes et épurées de la ville d'Ouargla. Possibilité de leur valorisation en irrigation; Larhyss Journal, ISSN 1112-3680, pp. 247-258
- PAEPA (2015) à Moundou :** Un Pas Vers un Avenir Durable. Disponible sur <https://tchadvision.com/moundou-les-chefs-de-quartiers-outilles-pour-une-meilleure-gestion-de-leau-et-de-lassainissement>. Consulté le 24/05/2025
- Paul, B., Martial D., Philippe O., (1969).** Nouvelles données sur les caractéristiques

chimiques et isotopiques des eaux du complexe quaternaire de la région de Thonon- les-Bains (Haute-Savoie). *Revue de géographie alpine*, 57(4), 823-830.

Photo D., Allahdin O., Biteman Ol., Akpekabou B., Poumaye N., (2022). Contribution à l'évaluation de la qualité des eaux de forage des régions de la Lobaye et Ombella Mpoko dans le SudOuest de la République Centrafricaine. *Journal de la pollution environnementale et de la santé humaine*, vol. 10, n° 1, 1322.

SDEA (2003). Schéma Directeur de l'Eau et de l'assainissement 2003-2020. Pour atteindre les objectif du millénaire et assurer une gestion intégrée et participative. Document principal Provisoire pour validation 1, 124p.

Schneider. J.L., (2001). Carte de valorisation des eaux souterraines A1: 1 500 000. Document DGDH, 706p.

Schneider, J.L. and Wolff, J.P. (1992). Carte géologique et Hydrogéologique au 1/1 500 000 de la République du Tchad. Mémoire explicatif. Document BRGM n° 209, Vol. 1, 2, 689 p

Seghir K., (2014). La vulnérabilité a la pollution des eaux souterraines de la région Tebessa-Hammamet (Est Algérien). *Larhyss Journal*, 18 : 53-61.

a case study of Kenya, Africa; Elsevier, Scientific African (2) e0 0 018, 13 p.

Siddick M. O., (2014). Mode d'alimentation en eaux dans les quartiers de la ville de N'Djaména. *Mémoire de Master*, Université de Yaoundé. 75P.

Sila,O.N. (2019). Physico-chemical and bacteriological quality of water sources in rural 10 settings,

Tomasbe E., (2015). Caractérisation physico-chimique des eaux souterraines de Moundou. *Mémoire de master en sciences de la terre*, Université de Dschang, 51p.

Tchadanaye N. M., Tarkodjiel M., (2009). Les tchadiens boivent des eaux troublées.

Tamonkem A. R., Kemgang D. T., Mvondo V. Y. E., Iwoudam M. E., Ngounou

N. B., (2024). Contribution of Piezometry and Hydro-Geochemistry to a Better Understanding of the Adamawa-Yadé Hard Rock Aquifer System in Ngaoundéré. *American Journal of Water Resources*.12(2) : 39-52.

Van der Gun, J. (2022). *Grands systèmes aquifères dans le monde entier*. Le projet sur les eaux souterraines. <https://doi.org/10.21083/978-1-77470-020-4>.

Vincent D., (2019). Société Française de médecine d'urgence. Disponible sur <http://www.sfm.org/toxin/Eau/parametres/Nitrite.HTM>. Consulté le 26/02/2025

Who (2011) Water Quality and Water borne disease in the Niger River Inland Delta, Mali: A study of local knowledge and response, Health and Place, vol.2, 2011, PP

White A.F., Blum A.E., Bullen T., (1999). The effect of temperature on experimental and natural chemical weathering rates of granitoid rocks. *Geochimica et Cosmochimica Acta*, 63 (19-20): 3277-3291.